Case Studies in Structural Engineering 6 (2016) 45–52

Contents lists available at ScienceDirect

Case Studies in Structural Engineering

journal homepage: www.elsevier.com/locate/csse

Fundamental period elongation of a RC building during the Pollino seismic swarm sequence

Maria Rosaria Gallipoli [a,*], Tony Alfredo Stabile [a], Philippe Guéguen [b], Marco Mucciarelli [c], Paolo Comelli [c], Michele Bertoni [c]

[a] Consiglio Nazionale delle Ricerche, Istituto di Metodologie per l'Analisi Ambientale, CNR-IMAA, Tito, PZ, Italy
[b] ISTerre, University J. Fourier/CNRS/IFSTTAR, Grenoble, France
[c] Istituto Nazionale di Oceanografia e Geofisica Sperimentale, Dipartimento Centro di Ricerche Sismologiche, OGS-CRS, Udine, Italy

ARTICLE INFO

Article history:
Received 17 January 2016
Received in revised form 12 April 2016
Accepted 22 May 2016
Available online 24 May 2016

Keywords:
Cost effective monitoring
Building period elongation
Non-stationary frequency response

ABSTRACT

A primary school in Rotonda was monitored during an on-going seismic sequence in the Pollino area, Southern Italy. The Reinforced Concrete (RC) building is a typical three story building with a concrete frame, bearing pre-cast slab flooring, concrete block internal walls and pre-cast external infill slabs. The monitoring began in September 2011 with a single station on top of the building, and after the $M_L = 5$ mainshock occurred in October 2012 a network was completed with accelerometers on each floor and real-time streaming data was transmitted to the Istituto Nazionale di Oceanografia e Geofisica Sperimentale (Udine-Northern Italy). The school suffered no visible damage during the sequence. The real-time monitoring of the Rotonda school proved to be important for two reasons: (1) the large range of magnitudes and recorded peak accelerations allowed the study of the non-stationary frequency response; (2) the results also show how a simple, real-time monitoring system using cost-effective accelerometers could be used as a tool to provide information on the damage state and usability of the school.

1. Introduction

Monitoring is an important tool for identification of the dynamic characteristics of a building and the estimation of their possible changes over time as a result of structural degradation due to earthquakes, aging and/or long-term, intense, operational demands. This approach is more important when considering the increasing number of aging structures and infrastructures, especially exposed to seismic prone activity for seismic risk. In the last two decades several innovative techniques have been proposed to identify the dynamic characteristics of real engineering structures [1–15]. Fast monitoring procedures are gaining ground; they obtain useful information about the extent of damage in a large number of strategic buildings during and after seismic events by using the records from a limited number of sensors located in the structure. According to Non-destructive Damage Evaluation (NDE) methods, the monitoring of the Rotonda building is a I level application, i.e. a method that only assesses if some damage has occurred. This monitoring gave us the opportunity to study the dynamic behaviour and the variation of the fundamental period due to different levels of motion of earthquakes before any damage; this building was not damaged, not even by the main shock ($M_L = 5$). Many recent experimental studies ([16,17] and

* Corresponding author at: National Research Council of Italy-IMAA, C.da S. Loja, 85050 Tito Scalo, PZ, Italy.
E-mail address: mariarosaria.gallipoli@imaa.cnr.it (M.R. Gallipoli).

http://dx.doi.org/10.1016/j.csse.2016.05.005

reference therein) have demonstrated the ability of ambient vibration surveys to estimate the main frequencies of building vibration in the elastic domain. Then, the important issue is to know how the fundamental frequency drop observed during weak to strong earthquake could be considered as a proxy of the damage. Observations about the fundamental frequency variation due to damage can be traced back both to Clinton et al. [18], for the Millikan Library buildings which has experienced several earthquakes, and to Dunand et al. [19] who studied some buildings during the 2003 Boumerdès earthquake. From weak to strong motion, Hans et al. [20] and Michel et al. [21,22] have reported the variation of the fundamental frequency of buildings related to the opening of cracks in the elastic domain. Such nonlinearities may produce a recoverable frequency decrease of about 35% during excitation. On the other hand, it seems that a 60% permanent drop in frequency is a limit before the collapse according to data compiled by Calvi et al. [23].

During the most recent Italian earthquakes particular attention was paid to study and assess the permanent and/or transient frequency drop in more detail in R.C. buildings. For example, the earthquakes recorded in the Navelli town hall during the 2009 Abruzzo earthquake reveal multiple temporary period elongations which did not correspond to an increase of damage (see for example Ref. [9]). In other cases, a permanent period shift accompanied by damage was observed during Molise earthquake, 2002 [24], Emilia earthquake, 2012 [25], in the above-mentioned cases the buildings had already suffered damage before the installation of the monitoring system. Dunand et al. [19], Ditommaso et al. [17] and Vidal et al. [26] have quantified the permanent period elongation related to different damage states on large sets of buildings during Boumerdes, Abruzzo and Lorca earthquakes respectively, in each case the period elongation for the red classified buildings being about 50–70%.

The monitoring of the Rotonda primary school provided the opportunity not only to study the non-stationary frequency response (during and after earthquakes), it also provided the Regional Civil Protection of Basilicata with information regarding the damage state and immediate occupancy of the building. The data was transmitted to the OGS Seismological Research Center (Udine-Northern Italy) in real time via the school internet connection, it was therefore possible to determine if each earthquake had caused damage related to permanent frequency drop monitoring. Moreover, during the monitoring the availability of co-located sensors with different characteristics allowed a comparison between the performances of electromechanical and MEMS accelerometers. It goes without saying that cost-effective instruments would allow a significant diffusion of the monitoring of buildings in real-time.

2. Seismological description of swarm

Since October 2010 a seismic swarm is affecting the Pollino mountain range. The sequence is still ongoing, with more than 2200 events with $M_L > 1.5$, of which about 700 were perceived by the population ($M_L > 2.0$). The spatial distribution of these events is in three clusters, the westernmost cluster was active during the three years, the middle cluster was activated in May 2012, and the easternmost cluster was activated by a 3.4 aftershock on December 19, 2012. Rotonda is at the Northern edge of the westernmost cluster, which is also the more active. The time occurrence of the earthquakes is also by clusters, whose inter-distance in time decreased by half each cluster for two years, until a $M_L = 5.0$ event took place on October 26, 2012 (Fig. 1). The sequence has not stopped since then, it is still producing events greater than $M_L = 1.5$ at a rate 10 time larger than the period prior to Autumn 2010 (see Fig. 2). The Pollino sequence appears to be peculiar for duration and productivity since when there is a good instrumental coverage of Italian seismicity, even if the swarm-like behaviour appears to be a characteristic feature of this mountain range (see Ref. [27]).

3. Description of the building monitoring

In September 2011, we installed one ETNA-Kinemetrics accelerometer in stand-alone configuration with local data storage on the second floor of the building (see Fig. 3; geographic coordinates: Lat = 39.94938 °N; Lon = 16.04157° E). The data was recorded at 200 samples per second (sps). The NS and EW components of the accelerometer were oriented along the transversal and the longitudinal directions with respect to the main axes of the structure, respectively. We collected in this first acquisition stage 6 foreshocks with $3.0 \leq M_L \leq 3.6$, the mainshock ($M_L = 5.0$), and 7 aftershocks with $2.8 \leq M_L \leq 3.3$, as reported in Table 1.

From 9 November, 2012 to 9 January, 2013 we updated the acquisition by installing a triaxial GeoSIG accelerometer along the vertical on each floor of the building as indicated in Fig. 3a (station G5 on the ground floor, station G4 at the first floor, and station G3 at the second floor that substituted the ETNA accelerometer). The GeoSIG accelerometers have been developed during a project carried out by the Geological Survey of Canada [28] and are based on low cost, three-components and strong motion sensors (i.e. solid state micro electro mechanical systems, MEMS). The accelerometer was then manufactured and distributed by GeoSIG Ltd. The new configuration along the vertical with the same position at each floor was chosen to allow for a better monitoring of the building due to the possibility of: 1) allowing us the continuous recording of data and their transmission instead of triggering and manual retrieving; 2) performing Standard Spectral Ratio analysis from basement to top recordings instead of Horizontal-to-Vertical Spectral Ratio from single station; 3) studying the modal shape. In this paper we describe the improvement and the results of item 1). During this second stage, accelerometric data was continuously recorded at 100 sps for two months until 9 January 2013. The ETNA and GeoSIG accelerometers were oriented along the transversal and the longitudinal directions with respect to the main axes of the structure. In particular, we only selected the recordings of events with magnitude $M_L \geq 2.5$ from the continuous data of GeoSIG sensors (see Table 1). The hypocentral

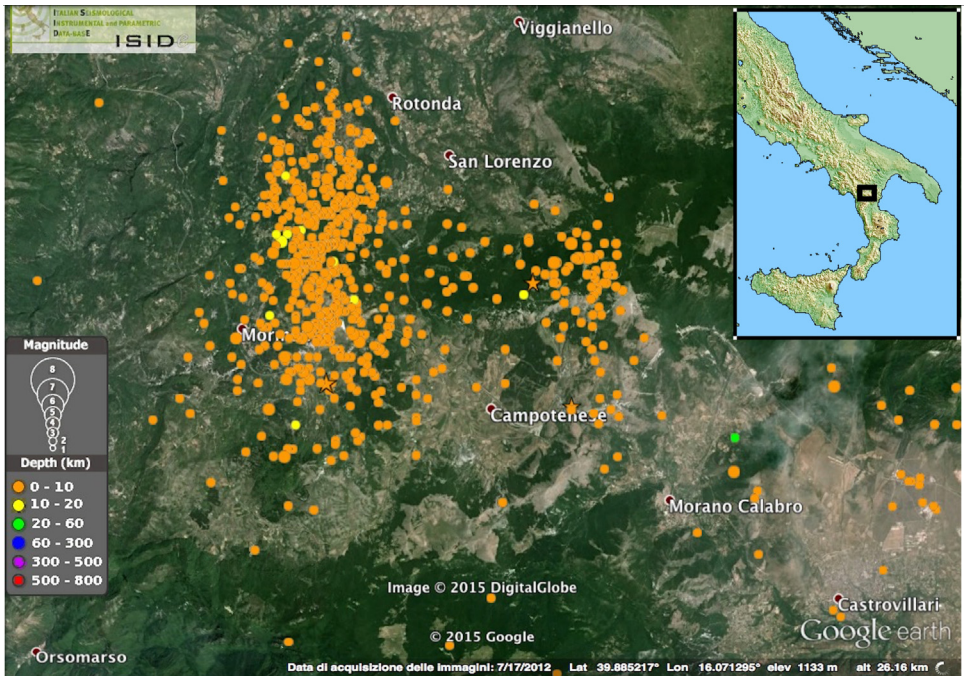

Fig. 1. The spatial distribution of Pollino seismic swarm. Only the events with $M_L > 2$ are plotted, with the large star indicating the $M_L = 5$ quake and smaller star the events with $M_L > 4$. Data is taken from the INGV ISIDE database (http://iside.rm.ingv.it/).

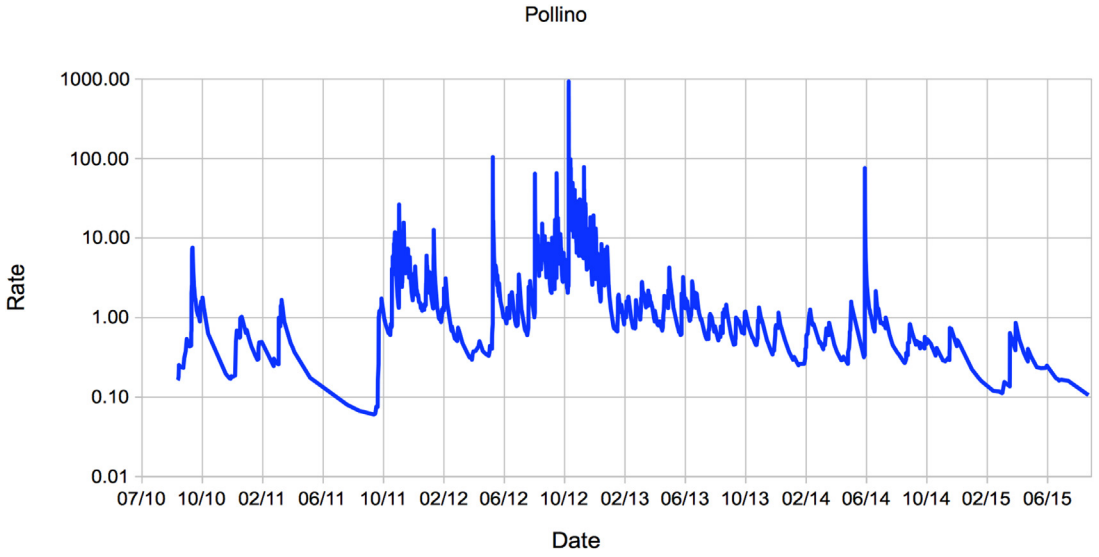

Fig. 2. The equivalent activity rate of the Pollino swarm (events per day), for earthquakes with magnitude greater or equal to 1.5. The maxima coincide with the largest events of the sequence and their aftershocks.

distances of the analysed foreshocks and aftershocks ranged from 6.6 km to 19.3 km, with peak acceleration on top of the building (PTA) between 0.003 and 0.07 g, whereas the hypocentre of the $M_L = 5.0$ earthquake was at 10.6 km distance from the building with PTA of 0.6 g.

4. Inter-event main period elongation

The acceleration response spectra were evaluated for all the 6 foreshocks, the main event, and all the 7 aftershocks recorded by the ETNA-Kinemetrics accelerometer (Table 1). Fig. 4 shows the acceleration response spectra at 5% damping along the transversal and the longitudinal directions. It is possible to observe that the response spectra shapes of foreshocks

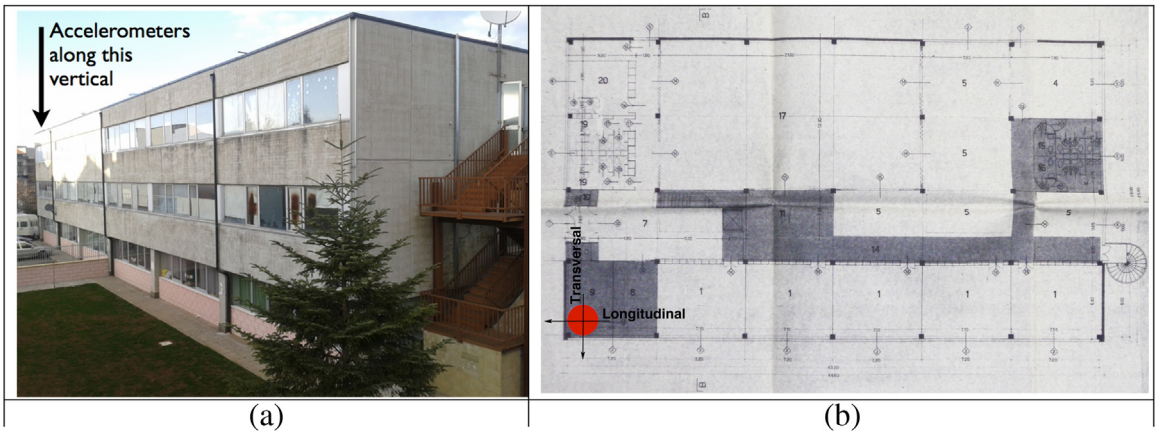

Fig. 3. (a) The building hosting the school in Rotonda indicating the vertical along which the accelerometers were installed. (b) Plan of the building indicating the position of the accelerometers (red circle) and their orientation (arrows) (for interpretation of the references to colour in this figure legend, the reader is referred to the web version of this article).

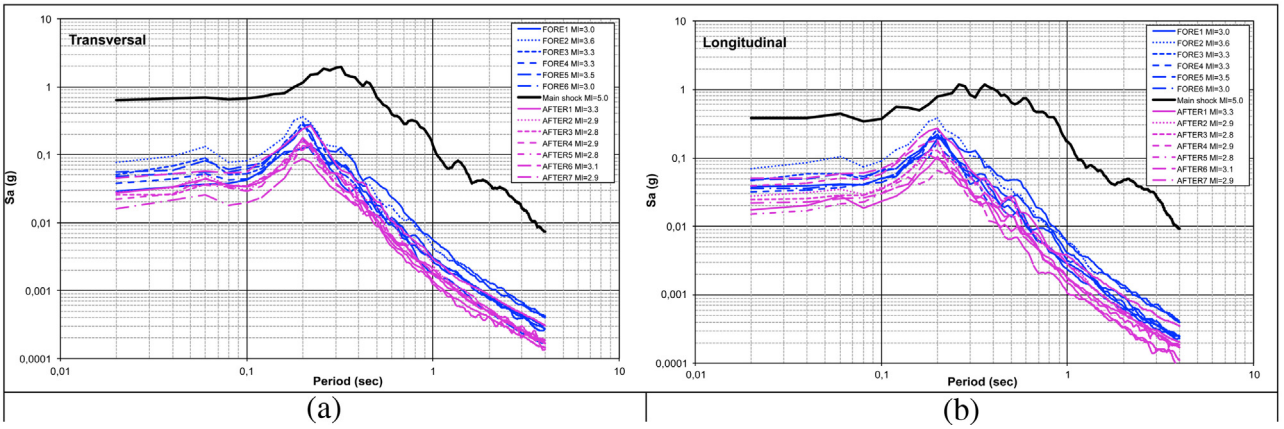

Fig. 4. Acceleration response spectra evaluated for 6 foreshocks (blue), the main event (black), and 7 aftershocks (pink) along the transversal (a) and the longitudinal (b) directions (for interpretation of the references to colour in this figure legend, the reader is referred to the web version of this article).

and aftershocks have similar behaviour with fundamental period at about 0.2 s, whereas the response spectra of the main event has fundamental peaks at 0.3 s along the transversal direction and a broad peak at 0.3-0.4 s along the longitudinal direction. The period elongation was observed only during the main shock, returning afterwards to 0.2 s; then we can deduce that the building had only a transient elongation of its fundamental period, without permanent changes.

The period variation *vs* peak acceleration recorded on top of the building was reported using ETNA-Kinemetrics data, shown in Fig. 5. The accelerations and the variations of period were selected on the window corresponding to 5%-95% of Arias intensity. For peak acceleration ranging between 0.1-0.6 m/s^2 there is period variation comprised within 10%, on the contrary a period increase of approximately 50% was observed during the main shock (PTA > 1 m/s^2).

5. Intra-event main period variation

It is important to study the intra-event main period variation to have a first hint about the possible onset of the damage of the building. This requires the use of time-frequency distribution methods to evaluate the variation of the building period during the recordings of shocks. A method widely used in the past was the Short-Time Fourier Transform (see e.g. Ref. [29]). More recently, different approaches were proposed to increase the precision in the estimate of the period distribution at any given instant in time domain, allowing for a better characterization of period variation in time. In this way it is possible to follow temporary and permanent period variation of the principal modes of the building, to be compared with the range of variation associated to absence of damage or the onset of non-structural/structural damage.

In this study we evaluate the mainshock using two time-frequency distribution methods recently proposed: the Smoothed Pseudo Wigner–Ville Distribution [30] and S-transform [31]. Fig. 6 shows the Smoothed Pseudo Wigner–Ville Distribution during the mainshock (M_L = 5.0) evaluated between 3 and 6 Hz along transversal and longitudinal components, while Fig. 7

Table 1
List of recorded events with the mainshock highlighted in grey. The last column indicates the sensor used for the acquisition.

Date	Origin Time (UTC)	Latitude (°N)	Longitude (°E)	Depth (km)	Magnitude M_L	Sensor
28/09/2012	5:56:46	39.912	16.087	3.0	3.0	ETNA
01/10/2012	21:27:51	39.903	16.010	7.9	3.3	ETNA
01/10/2012	20:28:28	39.901	16.013	8.1	3.6	ETNA
02/10/2012	0:08:57	39.906	16.019	7.4	3.3	ETNA
18/10/2012	2:51:57	39.887	16.034	7.8	3.5	ETNA
23/10/2012	10:40:24	39.906	16.021	9.2	3.0	ETNA
25/10/2012	23:16:01	39.895	16.012	8.3	3.3	ETNA
25/10/2012	23:05:24	39.881	16.009	6.3	5.0	ETNA
26/10/2012	2:25:09	39.920	16.032	6.6	2.9	ETNA
27/10/2012	2:42:20	39.932	16.025	8.5	2.8	ETNA
28/10/2012	13:52:18	39.920	15.987	8.9	2.9	ETNA
28/10/2012	3:37:46	39.925	16.007	8.8	3.1	ETNA
28/10/2012	3:09:17	39.912	16.015	9.6	2.8	ETNA
28/10/2012	0:30:44	39.932	16.004	9.4	2.9	ETNA
09/11/2012	20:27:15	39.932	16.022	8.2	2.6	GeoSIG
11/11/2012	20:31:51	39.916	15.990	9.0	2.5	GeoSIG
12/11/2012	3:03:53	39.920	15.999	10.0	2.8	GeoSIG
15/11/2012	12:16:54	39.923	16.011	9.1	2.7	GeoSIG
16/11/2012	19:40:48	39.881	16.009	7.4	2.9	GeoSIG
21/11/2012	6:43:25	39.938	16.011	5.3	2.9	GeoSIG
22/11/2012	18:42:54	39.928	15.999	9.8	2.5	GeoSIG
22/11/2012	15:32:16	39.941	16.018	9.0	2.6	GeoSIG
22/11/2012	1:59:52	39.921	16.030	9.0	3.3	GeoSIG
23/11/2012	16:24:13	39.915	16.000	10.5	2.6	GeoSIG
24/11/2012	22:24:26	39.914	16.015	8.9	2.7	GeoSIG
24/11/2012	21:05:23	39.917	16.019	8.9	2.5	GeoSIG
24/11/2012	16:25:09	39.872	15.978	8.8	2.7	GeoSIG
25/11/2012	20:41:11	39.909	16.009	8.9	3.0	GeoSIG
25/11/2012	17:48:02	39.916	16.008	9.8	3.2	GeoSIG
25/11/2012	16:23:41	39.916	16.004	9.9	2.5	GeoSIG
25/11/2012	11:26:28	39.915	16.011	9.2	2.7	GeoSIG
25/11/2012	8:53:33	39.887	16.017	10.6	2.9	GeoSIG
25/11/2012	8:42:25	39.911	16.015	6.9	2.9	GeoSIG
25/11/2012	8:36:49	39.917	16.022	8.3	2.5	GeoSIG
25/11/2012	8:30:31	39.917	16.009	9.7	2.6	GeoSIG
25/11/2012	8:28:39	39.921	16.027	7.5	3.7	GeoSIG
26/11/2012	23:44:11	39.906	16.015	9.9	2.9	GeoSIG
26/11/2012	1:27:57	39.931	16.015	7.3	2.6	GeoSIG
28/11/2012	12:37:31	39.927	16.020	5.8	3.1	GeoSIG
28/11/2012	2:43:46	39.929	16.000	8.2	3.0	GeoSIG
29/11/2012	19:43:22	39.929	16.020	6.9	2.5	GeoSIG
30/11/2012	03:03:44	39.923	16.025	5.1	3.2	GeoSIG
01/12/2012	4:43:02	39.920	16.039	6.3	2.8	GeoSIG
05/12/2012	12:25:02	39.933	16.009	8.4	2.6	GeoSIG
06/12/2012	23:27:10	39.926	16.028	8.1	2.8	GeoSIG
06/12/2012	14:23:52	39.946	16.025	8.1	2.6	GeoSIG
11/12/2012	14:28:43	39.888	16.017	10.0	3.4	GeoSIG
13/12/2012	04:44:03	39.906	16.036	7.7	3.0	GeoSIG
15/12/2012	04:20:05	39.863	16.035	5.1	2.6	GeoSIG
18/12/2012	11:05:43	39.838	16.172	9.2	2.8	GeoSIG
18/12/2012	11:03:18	39.841	16.167	8.1	3.4	GeoSIG
29/12/2012	7:12:02	39.906	16.022	10.0	2.7	GeoSIG
09/01/2013	15:05:27	39.901	16.016	9.0	2.6	GeoSIG

displays the S-transform of the mainshock evaluated up to 10 Hz along the same components, whose recording is visible in the lower panel. The transient variation of period is more evident in the longitudinal component and much more defined using the Smoothed Pseudo Wigner–Ville Distribution technique. During the main amplitude of S-waves there is a decrease of the main frequency to 2–3 Hz (periods of about 0.3-0.5 s) along the longitudinal direction and down to 3 Hz (periods of about 0.3 s) along the transversal direction, however during the coda the main frequency returns to the initial values of 5 Hz (periods of 0.2 s). The results obtained shows the period elongation of about 50% in the longitudinal direction and of about

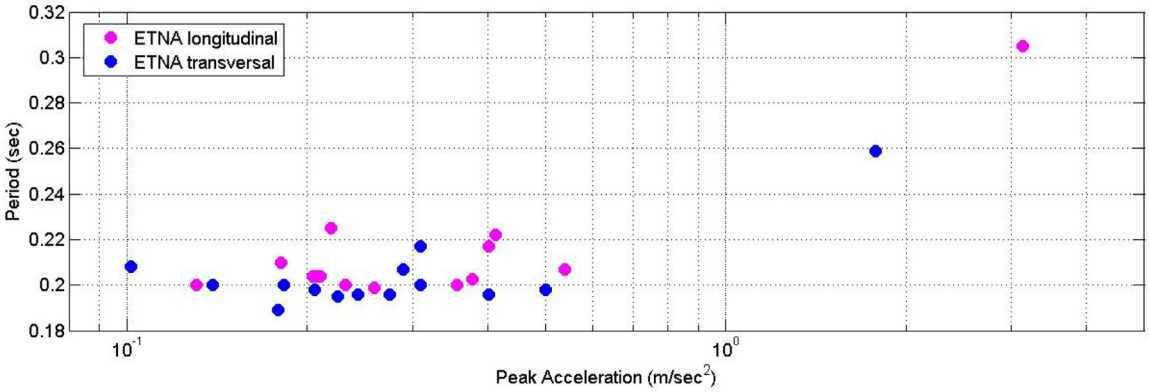

Fig. 5. Period variation *vs* peak acceleration using ETNA-Kinemetrics data.

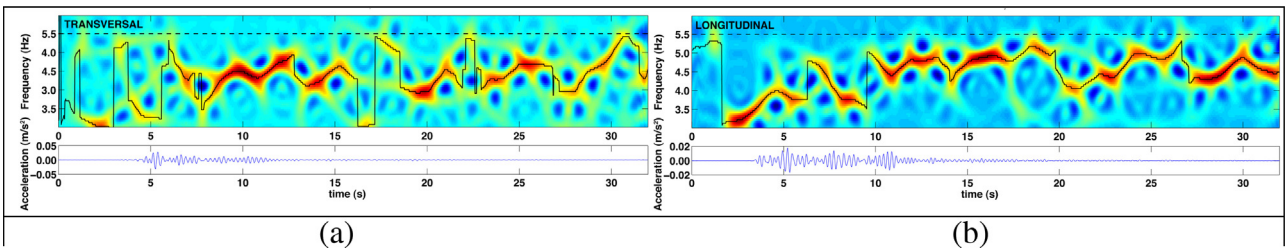

Fig. 6. Smoothed Pseudo Wigner–Ville Distribution of the mainshock evaluated between 3 and 6 Hz along the transversal (a) and the longitudinal (b) components.

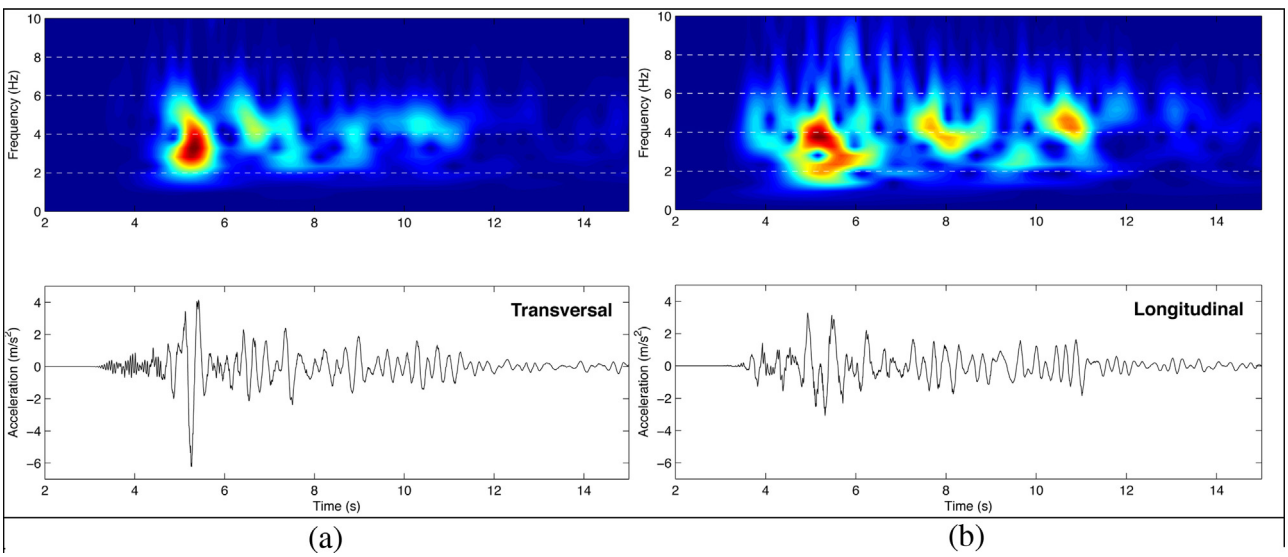

Fig. 7. S-transform of the mainshock evaluated up to 10 Hz along the transversal (a) and the longitudinal (b) components.

30% in the transversal one during the strong motion, but it has to be considered as purely transient, since the fundamental period of the building was already recovered during the coda. After 30 s, we observe that the recovery is not complete and a shift of frequency exists compared to the pre-event frequency (indicated by dashed line in Fig. 6). Without continuous data available at the time of recording, it is not possible to give a full assessment of the immediate occupancy criteria based only on this data. Anyway after the main shock, the fundamental period computed on the first aftershock is equal to the period

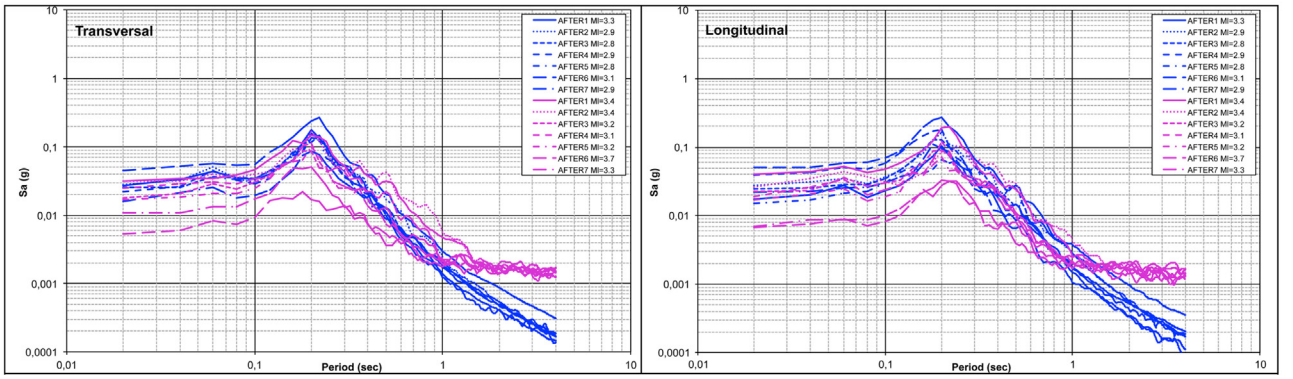

Fig. 8. Comparison between acceleration response spectra evaluated for 7 aftershocks recorded by the ETNA sensor (blue curves) and 7 aftershocks recorded by the GeoSIG sensor (violet curves). For periods longer than about 1.0 s the GeoSIG response spectra become flat along both the transversal (left) and the longitudinal (right) components (for interpretation of the references to colour in this figure legend, the reader is referred to the web version of this article).

obtained from foreshocks, allowing us to conclude the building is safe. But the time required to give this information is not immediate and continuous recording is better for deriving information related to immediate occupancy to decision makers.

6. Comparisons between GeoSIG and electromechanical accelerometers

The availability of co-located sensors with different characteristics allowed for a comparison of the GeoSIG and force-balance accelerometers performances. The GeoSIG is a project developed by the Geological Survey of Canada [28] based on low cost three-components, i.e. solid state micro electro mechanical (MEMS) strong motion sensors. The accelerometer was then manufactured and distributed by GeoSIG Ltd. The GeoSIG sensor installed in the school had a nominal sensitivity of 0.001 g. According to D'Alessandro and D'Anna [32] the MEMS accelerometer has excellent frequency and phase response, comparable with that of some standard force-balance accelerometers produced for strong-motion seismology in the typical frequency and amplitude range of interest of earthquake engineering (0.2–20 Hz and 10–2000 mg) but the main drawback is its low sensitivity, due to the high instrumental self noise, and so it can be used effectively only to record moderate and strong earthquakes (M_L >5) near the epicentral area.

We analysed the recordings of 39 aftershocks with a magnitude of $M_L \geq 2.5$ (Table 1) acquired by the GeoSIG and force-balance accelerometers. As an example, Fig. 8 shows the acceleration response spectra of the seven aftershocks recorded by ETNA accelerometers and seven aftershocks with similar magnitude, distance and PTA recorded by GeoSIG. The comparison shows that the SNR declines at a slightly higher value, just below Sa = 0.002 g (flat trend). The acceleration spectral value is reached for a period of 1 s. Considering that the fundamental frequency of the building is five times higher and the spectral ordinates are about hundred times higher, this could be considered satisfactory for the purpose of monitoring the studied building.

7. Conclusions

During the Pollino (Southern Italy) seismic swarm we installed inside the Rotonda school a monitoring system with real time data transmission that was set up in a short time after the mainshock, substituting a pre-existing single station, trigger monitoring. Permanent instrumentation can then provide relevant detection of changes based on observation of period elongation. It was then possible for Civil Protection authorities to gain useful information in deciding if a building is safe for use, requires inspections or has to be abandoned, according to the three thresholds usually adopted after earthquake crisis for building inventory. This requires a continuous recording also since the frequency recovery may be long, that may also provide false alarm situation if the interpretation of the period elongation is not complete.

The building in Rotonda provided another very important result in the discussion about the importance of temporary *vs* permanent period elongation for damage assessment. The building suffered during the mainshock a spectral acceleration at the top floor reaching almost 2 g, which caused a period elongation of about 50% that was completely recovered at time of the first recorded aftershock three hours later and thus has to be considered a purely temporary variation. Since post-event, on-site verification showed that the building suffered no damage, this suggests that to testify onset of damage, the presence of a permanent variation seems to be more important than a temporary variation even if it is a large one. Finally, cost-effective MEMS accelerometers proved to be reliable for the identification of main dynamic parameters of buildings even when weak ground motion occurs (below 0.01 g) and for relatively stiff buildings (frequency >1 Hz). We hope that this could open the way to a widespread, real-time building monitoring in the same way that MEMS based instruments are now used to build extra-dense networks to map ground shaking in California [33] and in New Zealand [34]. A first attempt of cost-effective

accelerometric monitoring of strategic building for civil protection purpose will start this year in the North-Eastern region of Italy ([35]).

References

[1] S.S. Ivanovic, M.D. Trifunac, M.I. Todorovska, On identification of damage in structures via wave travel times, in: M. Erdik, M. Celebi, V. Mihailov, N. Apaydin (Eds.), Proc. NATO Advanced Research Workshop on Strong-Motion Instrumentation for Civil Engineering Structures, June 2–5, 2001, Istanbul, Turkey, Kluwer Academic Publishers, 1999, p. 21.
[2] R. Snieder, E. Safak, Extracting the building response using seismic interferometry: theory and application to the millikan library in Pasadena, California, Bull. Seism. Soc. Am. 96 (2006) 586–598.
[3] M.I. Todorovska, M.D. Trifunac, Impulse response analysis of the Van Nuys 7-storey hotel during 11 earthquakes and earthquake damage detection, Struct. Control. Health Monit. 15 (2008) 90–116.
[4] M.I. Todorovska, M.D. Trifunac, Earthquake damage detection in structures and early warning, in: The 14th World Conference on Earthquake Engineering. October 12–17, Beijing, China, 2008.
[5] M.I. Todorovska, M.D. Trifunac, Earthquake damage detection in the Imperial County Services Building III: analysis of wave travel times via impulse response functions, Soil Dyn. Earthq. Eng. 28 (5) (2008) 387–404.
[6] M.I. Todorovska, Seismic interferometry of a soil-structure interaction model with coupled horizontal and rocking response, Bull. Seism. Soc. Am. 99 (2009) 611–625.
[7] M.I. Todorovska, Soil-structure system identification of Millikan Library North-South response during four earthquakes (1970–2002): what caused the observed wandering of the system frequencies? Bull. Seism. Soc. Am. 99 (2009) 626–635.
[8] M.D. Trifunac, M.I. Todorovska, M.I. Manic, B. Bulajic, Variability of the fixed-base and soil structure system frequencies of a building—the case of Borik-2 building, Struct. Control Health Monit. 17 (2010) 120–151.
[9] M. Mucciarelli, M. Bianca, R. Ditommaso, M.R. Gallipoli, A. Masi, S. Parolai, M. Picozzi, C. Milkereit, M. Vona, Far field damage on RC buildings: the case study of the Navelli during the L'Aquila (Italy) seismic sequence 2009, Bull. Earthq. Eng. 9 (2011) 263–283.
[10] M. Picozzi, R. Ditommaso, S. Parolai, M. Mucciarelli, C. Milkereit, M. Sobiesiak, D. Di Giacomo, M.R. Gallipoli, M. Pilz, M. Vona, J. Zschau, Real time monitoring of structures in task-forcemissions: the example of theMw = 6.3 Central Italy Earthquake, April 6, 2009, Nat. Hazards 52 (2010) 253–256.
[11] Roshanak Omrani, Ralph E. Hudson, Ertugrul Taciroglu, Story-by-story estimation of the stiffness parameters of laterally-torsionally coupled buildings using forced or ambient vibration data: I. Formulation and verification, Earthq. Eng. Struct. Dyn. 41 (2012) 1609–1634.
[12] Roshanak Omrani, Ralph E. Hudson, Ertugrul Taciroglu, Story-by-story estimation of the stiffness parameters of laterally-torsionally coupled buildings using forced or ambient vibration data: II. Formulation and verification, Earthq. Eng. Struct. Dyn. 41 (2012) 1635–1649.
[13] S. Bisht Saurabh, P. Singh Mahendra, Detecting sudden changes in stiffness using high-pass filters, Struct. Control Health Monit. 19 (2012) 319–331.
[14] H.M. Dinh, T. Nagayamaz, Y. Fujinoy, Structural parameter identification by use of additional known masses and its experimental application, Struct. Control Health Monit. 19 (2012) 436–450.
[15] R. Ditommaso, M. Mucciarelli, F.C. Ponzo, Analysis of non-stationary structural systems by using a band-variable filter, Bull. Earthq. Eng. 10 (2012) 895–911.
[16] M.R. Gallipoli, M. Mucciarelli, M. Vona, Empirical estimate of fundamental frequencies and damping for Italian buildings, Earthq. Eng. Struct. Dyn. 38 (2009) 973–988.
[17] R. Ditommaso, M. Vona, M.R. Gallipoli, M. Mucciarelli, Evaluation and considerations about fundamental periods of damaged reinforced concrete buildings, Nat. Hazards Earth Syst. Sci. 13 (2013) 1903–1912.
[18] J.F. Clinton, S.C. Bradford, T.H. Heaton, J. Favela, The observed wander of the natural frequencies in a structure, Bull. Seismol. Soc. Am. 96 (2006) 237–257.
[19] F. Dunand, P. Guéguen, P.Y. Bard, J. Rodgers, M. Celebi, Comparison of the dynamic parameters extracted from weak, moderate and strong building motion, in: Proceedings of the 1 St European Conference of Earthquake Engineering and Seismology, Number1021, Geneva, Switzerland, 6–8 September, 2006.
[20] S. Hans, C. Boutin, E. Ibraim, P. Roussillon, In situ experiments and seismic analysis of existing buildings. Part I: experimental investigations, Earthq. Eng. Struct. Dyn. 34 (2005) 1513–1529.
[21] C. Michel, P. Guéguen, P.Y. Bard, Dynamic parameters of structures extracted from ambient vibration measurements: an aid for the seismic vulnerability assessment of existing buildings in moderate seismic hazard regions, Soil Dyn. Earthq. Eng. 28 (8) (2008) 593–604.
[22] C. Michel, P. Guéguen, S. El Arem, J. Mazars, P. Kotronis, Full-scale dynamic response of an RC building under weak seismic motions using earthquake recordings, ambient vibrations and modelling, Earthq. Eng. Struct. Dyn. 39 (4) (2010) 419–441.
[23] G.M. Calvi, R. Pinho, H. Crowley, State-of-the-knowledge on the period elongation of RC buildings during strong ground shaking, in: First European Conference on Earthquake Engineering and Seismology, Geneva, 2006 (CD paper number 1535).
[24] M. Mucciarelli, M.R. Gallipoli, A. Masi, M. Vona, F. Ponzo, M. Dolce, Analysis of RC building dynamic response and soil-building resonance based on data recorded during a damaging earthquake (Molise, Italy 2002), Bull. Seismol. Soc. Am. 94 (5) (2004) 1943–1953.
[25] A. Masi, G. Santarsiero, M.R. Gallipoli, M. Mucciarelli, V. Manfredi, A. Dusi, T.A. Stabile, Performance of the health facilities during the 2012 Emilia (Italy) earthquake and analysis of the Mirandola hospital case study, Bull. Earthq. Eng. 12 (5) (2014) 2419–2443.
[26] F. Vidal, M. Navarro, C. Aranda, T. Enomoto, Changes in dynamic characteristics of Lorca RC buildings from pre- and post-earthquake ambient vibration data, Bull. Earthq. Eng. 12 (5) (2014) 2095–2110.
[27] A. Tertulliani, L. Cucci, New insights on the strongest historical earthquake in the pollino region (Southern Italy), Seismol. Res. Lett. 85 (3) (2014) 743–751.
[28] A. Rosenberg, K. Beverley, G. Rogers, The new strong motion seismic network in southwest British Columbia, in: Canada 13th World Conference on Earthquake Engineering, Vancouver, B.C., Canada, August 1–6, 2004 (Paper No. 3373).
[29] M. Mucciarelli, A. Masi, M.R. Gallipoli, P. Harabaglia, M. Vona, F. Ponzo, M. Dolce, Analysis of RC building dynamic response and soil-building resonance based on data recorded during a damaging earthquake (Molise, Italy, 2002), Bull. Seismol. Soc. Am. 94 (5) (2004) 1943–1953.
[30] C. Michel, P. Guéguen, Time-Frequency analysis of small frequency variations in civil engineering structures under weak and strong motions using a reassignment method, Struct. Health Monit. 9 (2010) 159–171.
[31] R.G. Stockwell, L. Mansinha, R.P. Lowe, Localization of the complex spectrum: the S transform, IEEE Trans. Signal Process 44 (1996) 998–1001.
[32] A. D'Alessandro, G. D'Anna, Suitability of low-Cost three-Axis MEMS accelerometers in strong-Motion seismology: tests on the LIS331DLH (iPhone) accelerometer, Bull. Seismol. Soc. Am. 103 (2013) 2906–2913.
[33] R.W. Clayton, M. Heaton Th Kohler, M. Chandy, R. Guy, J. Bunn, Community seismic network: a dense array to sense earthquake strong motion, Seism. Res. Lett. 86 (2015) 1354–1363, http://dx.doi.org/10.1785/0220150094.
[34] J.F. Lawrence, E.S. Cochran, A. Chung, A. Kaiser, C.M. Christensen, R.M. Allen, J.W. Baker, B. Fry, T. Heaton, D. Kilb, M.D. Kohler, M. Taufer, Rapid earthquake characterization using MEMS accelerometers and volunteer hosts following the M 7.2 Darfield, New Zealand, earthquake, Bull. Seismol. Soc. Am. 104 (1) (2014) 184–192.
[35] M. Mucciarelli, A new earthquake monitoring strategy in a cross-border seismic zone, in: P. Galea, R.P. Borg, D. Farrugia, M.R. Agius, S. D'amico, A. Torpiano, M. Bonello (Eds.), Proceeding of the International Conference Georisks in the Mediterranean and Their Mitigation, Malta 20–21, 2015, pp. 13–16, http://www.mistralservice.it/books/PDF/ProceedingsGEORISKS.pdf (access 12.04.16).